JLB

Article

p66Shc regulates vesicle-mediated secretion in mast cells by affecting F-actin dynamics

Giulia Masi, David Mercati,* Elisa Vannuccini,* Eugenio Paccagnini,* Maria Giovanna Riparbelli,* Pietro Lupetti,* Pier Giuseppe Pelicci,† Cosima T. Baldari,* and Cristina Ulivieri*,1*

*Department of Life Sciences, University of Siena, Italy; and †Department of Experimental Oncology, European Institute of Oncology, Milan, Italy

RECEIVED MARCH 27, 2013; REVISED AUGUST 29, 2013; ACCEPTED SEPTEMBER 5, 2013. DOI: 10.1189/jlb.0313178

ABSTRACT

The extracellular vesicular compartment has emerged as a novel system of intercellular communication; however, the mechanisms involved in membrane vesicle biogenesis and secretion are as yet unclear. Among immune cells releasing membrane vesicles—mast cells that reside near tissues exposed to the environment—are master modulators of immune responses. Here, we have addressed the role of p66Shc, a novel regulator of mast cell activation and homeostasis, in the dynamic reorganization of the actin cytoskeleton that is associated with morphological changes during secretion. We show that p66Shc is recruited as a complex with the lipid phosphatase SHIP1 to the F-actin skeleton and impairs antigen-dependent cortical F-actin disassembly and membrane ruffling through the inhibition of Vav and paxillin phosphorylation. We also show that in addition to acting as a negative regulator of antigen-dependent mast cell degranulation, p66Shc limits the basal release of granule contents by inhibiting microvesicle budding from the plasma membrane and piecemeal degranulation. These findings identify p66Shc as a critical regulator of actin dynamics in mast cells, providing a basis for understanding the molecular mechanisms involved in vesicle-mediated secretion in these cells.
***J. Leukoc. Biol.* 95: 285–292; 2014.**

Introduction

Antigen-induced aggregation of FcεRI, the high-affinity IgER expressed on mast cells, is required for the release of preformed and newly synthesized, proinflammatory mediators that ultimately give rise to allergic reactions [1]. Beside being key players in allergic inflammatory responses, mast cells control adaptive immune responses, thereby participating in host defense. Several mechanisms contribute to this function, including cell–cell interaction via membrane-associated receptors and release of cytokines and soluble mediators by degranulation, as well as through the release of membrane vesicles carrying a cargo of immunoregulatory molecules [2–4].

Two morphologically distinct degranulation pathways, namely anaphylactic degranulation and piecemeal degranulation, are believed to regulate the release of inflammatory mediators in mast cells [5]. During anaphylactic degranulation, which occurs following antigen stimulation through canonical exocytosis, cytoplasmatic granules rapidly fuse with each other and with the plasma membrane, resulting in a massive release of prestored mediators. Conversely, constitutive degranulation, also referred to as piecemeal degranulation, defines a peculiar release of granule materials in the absence of intergranule fusion or granule fusion with the plasma membrane. Cells undergoing piecemeal degranulation are identified by the presence of a mixture of granules with electron-dense content and empty granules and the so-called activated secretory granules further distinguished based on their content distribution, in haloed or semilunar-patterned granules [6]. In addition, mast cells release extracellular vesicles containing several mediators, which have emerged as key regulators of intercellular communication [4]. These include exosomes, i.e., vesicles of 50–100 nm in diameter that originate from MVBs and are released into the microenvironment following MVB fusion with the plasma membrane and larger vesicles of 100–1000 nm in diameter, referred to as microvesicles, that shed from mast cells by plasma membrane budding/blebbing [7–9]. The release of membrane vesicles into the extracellular space is dependent on the functional state of cells and contributes to the dynamic

Abbreviations: 3D=three-dimensional, BMMC=bone marrow-derived mast cell, DNP-ALB=albumin-conjugated dinitrophenyl, LatB=latrunculin B, MVB=multivesicular body, p66Shc$^{-/-}$=p66Shc-deficient, PIP3=phosphatidylinositol (3,4,5)-triphosphate, RBL=rat basophilic leukemia, SEM=scanning electron microscopy, Shc=Src homology and collagen, SHIP1=Src homology-containing inositol 5′ phosphatase-1, TEM=transmission electron microscopy

The online version of this paper, found at www.jleukbio.org, includes supplemental information.

1. Correspondence: Dept. of Life Sciences, University of Siena, Via Aldo Moro 2, 53100 Siena, Italy. E-mail: cristina.ulivieri@unisi.it

composition of the tissue microenvironment [10]; however, the mechanisms implicated in their biogenesis and secretion as well as their interaction with target cells are as yet unclear.

Rearrangements of the cytoskeleton represent the unifying feature of all secretion processes. In mast cells, changes in the microtubule and the actin cytoskeleton are required for the degranulation process [11–14], which can be dissected into two steps, i.e., microtubule-driven granule translocation to the plasma membrane and actin-dependent granule fusion with the plasma membrane. Actin-filament remodeling close to the plasma membrane is a fundamental step in mast cell secretion. Cortical actin filaments act as a barrier, made predominantly of actin and myosin, keeping apart the secretory granules from their fusion sites at the plasma membrane in the absence of stimulation [14, 15]. In agreement with a negative role for cortical F-actin during secretion, antigen-induced disassembly of the cortical F-actin network is required for mast cell exocytosis [14, 16]. These dynamic changes in the actin cytoskeleton, which include fragmentation and opening of large, subcortical areas devoid of F-actin, have been proposed to facilitate the access of vesicles to secretory sites, similar to neuroendocrine cells [17]. On the other hand, drug-induced depletion of actin filaments has been demonstrated to prevent antigen-dependent mast cell degranulation, suggesting that actin polymerization also plays a positive role during secretion [18]. Antigen-dependent exocytosis is indeed controlled by the activation of signaling pathways, which ultimately lead to de novo assembly of actin filaments around the secretory vesicle and at granule-docking sites [19, 20]. Whereas significant progress has been achieved in our understanding of the role of F-actin reorganization during mast cell secretion, the pathways that link FcεRI-dependent signaling to cytoskeleton dynamics remain to be elucidated.

Shc protein A belongs to the Shc family of adaptor proteins that regulate the signaling pathways, coupling a variety of cell-surface receptors to Ras activation [21]. We have shown recently that p66Shc, the longest of the three ShcA isoforms, is expressed in mast cells, where it attenuates FcεRI signaling by acting as an adapter to recruit the lipid phosphatase SHIP1 close to the plasma membrane. Accordingly, p66Shc$^{-/-}$ BMMCs exhibit increased responses, such as β-hexosaminidase and cytokine release, in the absence of stimulation and following FcεRI engagement [22].

Despite its identification as a negative regulator of FcεRI-dependent mast cell responses, to date, the impact of p66Shc on the cytoskeleton rearrangements required for degranulation has not been addressed. Here, we investigated the potential involvement of p66Shc in the cytoskeletal dynamics governing secretion. We show that BMMC generated from p66Shc$^{-/-}$ mice display enhanced FcεRI-mediated F-actin ring disassembly and membrane ruffling compared with WT BMMCs, which correlate with enhanced phosphorylation of Vav and paxillin. Interestingly, we found that p66Shc is recruited to the F-actin cytoskeleton, where it appears to stabilize SHIP1, thereby inhibiting antigen-induced actin remodeling. Moreover, we show that under basal conditions, p66Shc$^{-/-}$ in BMMC results in enhanced vesicle-mediated secretion and an altered pattern of cortical F-actin distribution.

MATERIALS AND METHODS

Cell activation

RBL-2H3 transfectants and BMMCs (see Supplemental material, Extended methods) were left untreated or sensitized with anti-DNP IgE 1 μg/ml for 1 h at 37°C and stimulated with DNP-ALB 100 ng/ml at 37°C for 5 or 20 min in TEM assay. In immunoprecipitation assays, cells were sensitized with anti-DNP IgE 1 μg/ml overnight at 37°C and stimulated with DNP-ALB 1 μg/ml for 5 min.

Lysis, immunoprecipitation, F-actin skeleton fractionation, and immunoblot assays

Cells (2×10^6/sample), left untreated or stimulated as described above in Cell activation, were lysed, as described elsewhere [22]. Alternatively, post-nuclear supernatants from 50×10^6 cells/sample were immunoprecipitated using rabbit anti-SHIP1 or anti-collagen homology 2 polyclonal antibodies and protein A-Sepharose (Amersham Biosciences, Buckinghamshire, UK). For the F-actin skeleton fractionation, 20×10^6 cells/sample were left untreated or stimulated as described above and processed as described [23]. Proteins were resolved by SDS-PAGE and transferred to nitrocellulose membranes (Protran; Whatman, GE Healthcare, Little Chalfont, Buckinghamshire, United Kingdom). Membranes were tested with the indicated antibodies, followed by HRP-conjugated secondary antibody (see Supplemental material, Extended methods). The relative phosphorylation/presence of each protein in each sample was normalized to its loading control, following quantitation of scanned immunoblots using ImageJ software. Data are presented as mean ± SD with the internal positive control of each set of samples taken as 100%.

SEM and TEM

Cells (1×10^5/sample) were seeded on poly-L-lysine-coated slides and processed for SEM microscopy. Alternatively cells (2×10^6/sample) were left untreated or stimulated as described above in Cell activation, pelleted at 176 *g* for 5 min, and processed for TEM microscopy (see Supplemental material, Extended methods).

Confocal microscopy

BMMCs and RBL-2H3 cells were seeded on poly-L-lysine-coated or uncoated slides, respectively, and then left untreated or primed as above. Cells were fixed 20 min in 4% PFA for F-actin or 10 min at −20°C in methanol for β-tubulin staining. Cells were then permeabilized with 0.01% Triton X-100 in PBS, supplemented with 1% BSA, and stained for 30 min at room temperature with TRITC-labeled phalloidin or overnight at 4°C with anti-β-tubulin antibody, followed by Alexa-Fluor 488 goat anti-mouse secondary antibody. Confocal laser-scanning microscopy was carried out on a Zeiss LSM700 (Zeiss, Oberkochen, Germany). Quantitation of the F-actin ring intensity was performed as described [24] (see Supplemental material, Extended methods).

Flow cytometry

Cells (2×10^5/sample) were left untreated or stimulated as described above in Cell activation, stained with TRITC-labeled phalloidin and analyzed in a FACScan flow cytometer (Becton Dickinson, San Jose, CA, USA).

Statistical analyses

Mean values, SD values, and Student's *t*-test (unpaired) were calculated using the Microsoft Excel application. A level of $P < 0.05$ was considered statistically significant (*P<0.05; **P<0.01; ***P<0.001). For BMMC, data were obtained from at least three independent p66Shc$^{-/-}$ or control BMMC cultures.

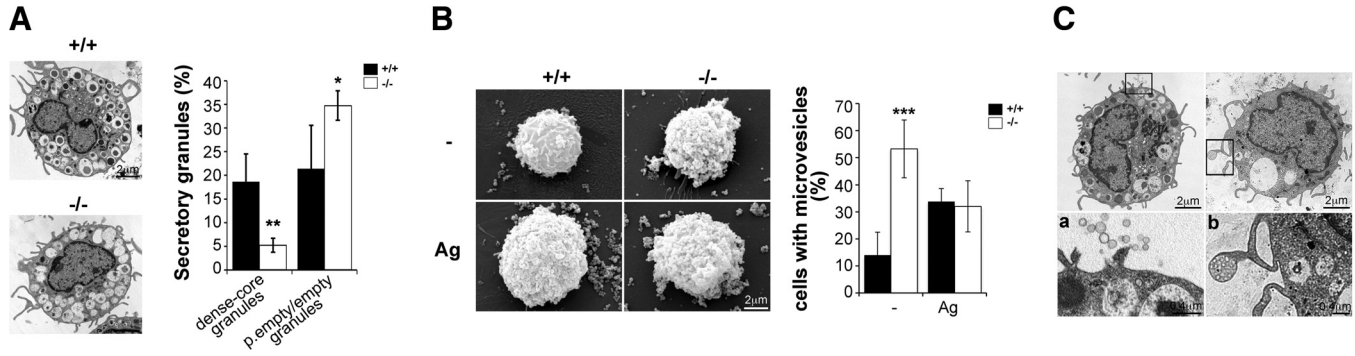

Figure 1. p66Shc controls the constitutive release of mediators by impairing piecemeal degranulation and release of microvesicles in mast cells. Representative TEM (A) and SEM (B) micrographs of control (+/+) and p66Shc$^{-/-}$ ($^{-/-}$) BMMCs, unstimulated (−) or sensitized with anti-DNP IgE and stimulated with DNP-ALB (Ag). The bar graphs show the percentage of dense-core and partially empty/empty granules (A) and the percentage of cells with extracellular microvesicles on their surface (B). Values are mean ± SD (n=2, 50 cells/sample for TEM, and n=2, 140 cells/sample for SEM). (C) Representative TEM micrographs of control BMMCs showing exosome release through exocytosis (left and a) or microvesicles (right and b). Magnifications of the regions delineated by the squares are also shown (n=2).

RESULTS AND DISCUSSION

p66Shc$^{-/-}$ alters granule ultrastructure in BMMCs

We have shown recently that p66Shc$^{-/-}$ BMMCs display enlarged toluidine blue-positive granules and substantial spontaneous degranulation compared with control BMMCs, indicating that p66Shc limits constitutive secretion in mast cells [22]. To gain further insight into the role of p66Shc in the process of constitutive secretion, we analyzed mast cell granules in WT and p66Shc$^{-/-}$ BMMCs by electron microscopy. As shown in **Fig. 1A**, resting BMMCs derived from WT mice show numerous electron-dense granules distributed homogeneously in the cytoplasm, whereas p66Shc$^{-/-}$ BMMCs have enlarged but fewer electron-dense granules. Interestingly, the lack of p66Shc results in a significant reduction in the number of dense-core granules (resting granules) and in an increase of large empty or partially empty granules (activated granules) compared with control cells (Fig. 1A, right). This suggests that p66Shc participates in mast cell homeostasis by controlling the constitutive release of mediators through piecemeal degranulation. Hence, the enlarged granules, documented in mast cells lacking p66Shc, using toluidine blue staining, which does not allow partially empty discrimination from dense-core granules, are likely to reflect the increase in the number of partially empty granules rather than an increase in mediator contents, as supported by the comparable cellular levels of β-hexosaminidase in BMMCs from control and p66Shc$^{-/-}$ mice [22].

p66Shc$^{-/-}$ BMMCs display enhanced, constitutive release of microvesicles

Upon activation, mast cells release, in addition to soluble mediators, small extracellular vesicles surrounded by a phospholipid bilayer, referred to as exosomes (50–100 nm) or microvesicles (100–1000 nm), which are generated by MVB exocytosis or plasma membrane budding/blebbing, respectively [8, 9, 25]. We investigated whether p66Shc$^{-/-}$ affects this process of mast cell secretion. An SEM analysis showed that, at variance with control BMMCs, in the absence of antigen stimulation, p66Shc$^{-/-}$ BMMCs were characterized by the presence of numerous extracellular microvesicles, both budding from the surface and dispersed around the cell, which fall into the size range of 100–1000 nm (Fig. 1B). The presence of these microvesicles on the cell surface was comparable between p66Shc$^{-/-}$ and control BMMCs following antigen stimulation (Fig. 1B). As the steady-state release of microvesicles is generally low, except for tumor cells [26], this result further supports the notion that p66Shc plays a crucial role in preventing constitutive vesicle budding from the plasma membrane.

The mechanism of extracellular vesicle generation is one of the features presently used to discriminate between exosomes and microvesicles [9]. Interestingly, the electron microscopy analysis revealed the presence, in a small proportion of BMMCs, of characteristic and previously unknown vesicles of 700–1500 nm, attached to protrusions originated from the plasma membrane and containing smaller, ~100-nm vesicles that are likely to be exosomes based on their size (Fig. 1C, b). These vesicles were observed independently of the activation state of BMMCs or the presence of p66Shc. Hence, in addition to classical exocytosis (Fig. 1C, a), the release of exosomes may occur through a novel mechanism involving bulk microvesicle budding from the plasma membrane.

p66Shc affects steady-state F-actin distribution and antigen-dependent submembranous F-actin disassembly and membrane ruffling in mast cells

In mast cells antigen-dependent secretion has been correlated with cortical F-actin depolymerization [14, 16, 27]. On the other hand, local actin assembly around the secretory vesicle during exocytosis has been reported [19], raising the question of the actual role of the actin cytoskeleton in the secretory process in mast cells. To evaluate whether p66Shc could affect mast cell degranulation, as well as microvesicle release, by acting on F-actin dynamics, cortical F-actin distribution and abundance were examined. p66Shc$^{-/-}$ and control BMMCs were left untreated or sensitized with IgE or stimulated with IgE/antigen, stained with TRITC-labeled phalloidin, and analyzed

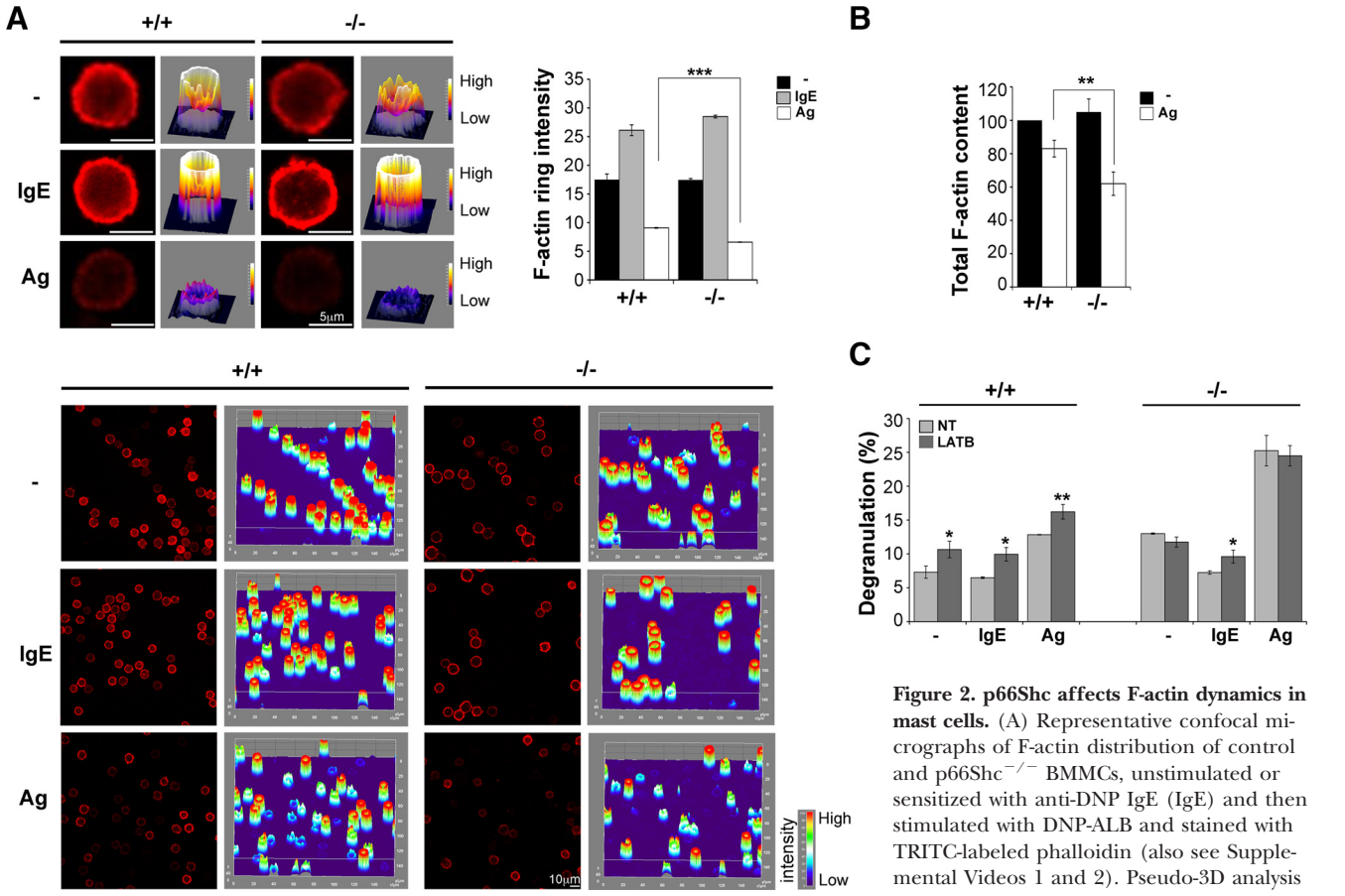

Figure 2. p66Shc affects F-actin dynamics in mast cells. (A) Representative confocal micrographs of F-actin distribution of control and p66Shc$^{-/-}$ BMMCs, unstimulated or sensitized with anti-DNP IgE (IgE) and then stimulated with DNP-ALB and stained with TRITC-labeled phalloidin (also see Supplemental Videos 1 and 2). Pseudo-3D analysis is also shown as an intensity plot. Graphs show a quantitation of the F-actin ring intensity (n=2, 200 cells/sample). (B) Flow cytometric analysis of total F-actin content in control and p66Shc$^{-/-}$ BMMCs, left untreated (black bars) or sensitized and stimulated as in A (white bars). Values are mean ± SD of the mean fluorescence intensity (untreated control cells taken as 100%; n=3). (C) β-Hexosaminidase release from control and p66Shc$^{-/-}$ BMMCs, stimulated as in A, untreated (NT; light-gray bars) or treated with LatB (LATB; dark-gray bars) (n=2; P=LatB vs. untreated). Values are mean ± SD.

by confocal microscopy (**Fig. 2A**). Measurement of the cortical fluorescence intensity showed that p66Shc does not alter F-actin ring intensity in resting conditions (Fig. 2A, upper). However, pseudo-3D analysis of F-actin intensity (Fig. 2A) highlighted a different distribution of F-actin-rich regions in resting p66Shc$^{-/-}$ and control BMMCs, with p66Shc$^{-/-}$ BMMCs displaying a more fragmented cortical F-actin ring, consistent with the enhanced basal secretion in p66Shc$^{-/-}$ cells [22]. In addition, an increased percentage of cells with the fragmented cortical F-actin ring was found in unstimulated p66Shc$^{-/-}$ BMMC (56% for p66Shc$^{-/-}$ vs. 22% for controls). The presence of numerous F-actin-free cortical regions in resting p66Shc$^{-/-}$ BMMCs compared with control cells is further evident in the 3D reconstruction of confocal images (see Supplemental Videos 1 and 2). Interestingly, treatment of p66Shc$^{-/-}$ BMMCs with IgE in the absence of antigen, which we have shown previously to reduce spontaneous degranulation to control levels [22], resulted in the recovery of a continous F-actin ring, similar to that observed in resting control cells (Fig. 2A). Consistent with the requirement for F-actin depolymerization for granule release [16], a significant decrease in cortical F-actin ring intensity (Fig. 2A) and total F-actin (Fig. 2B) was observed in p66Shc$^{-/-}$ and control BMMCs after antigen stimulation compared with their respective unstimulated controls. This decrease was, however, significantly more pronounced in p66Shc$^{-/-}$ BMMCs, supporting the notion that p66Shc acts as a negative regulator of antigen-dependent F-actin clearance occurring in mast cells following FcεRI triggering.

To analyze further the role of F-actin depolymerization in secretion and to assess the influence of p66Shc on F-actin dynamics, we measured β-hexosaminidase release in BMMCs pretreated with low doses of LatB, which is known to induce fragmentation of the cortical F-actin ring, thereby promoting degranulation [14]. LatB treatment resulted in a significant increase in basal and antigen-induced β-hexosaminidase release in control cells, whereas no effect was observed in p66Shc$^{-/-}$ BMMCs (Fig. 2C). Of note, in agreement with IgE-dependent enhancement in the cortical F-actin ring in BMMCs [16], treatment with IgE alone reduced spontaneous degranulation in p66Shc$^{-/-}$ and control BMMCs, an effect that was abrogated, to a large extent, by LatB. In support of a role of p66Shc in limiting F-actin reorganization and degranulation, pretreatment of a RBL-2H3 mast cell transfectant-expressing p66Shc with LatB rescued the p66Shc-dependent im-

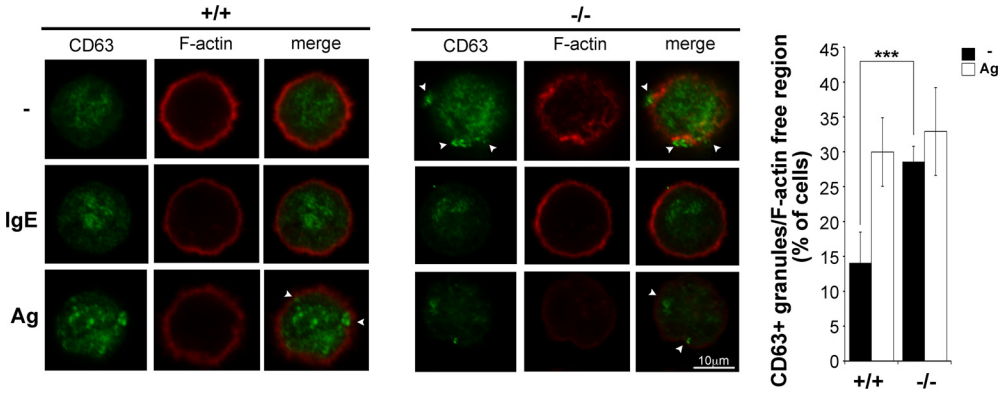

Figure 3. CD63$^+$ granules localize at cortical F-actin-free regions in p66Shc$^{-/-}$ BMMCs. Representative confocal micrographs of F-actin and CD63 distribution of control and p66Shc$^{-/-}$ BMMCs, unstimulated or sensitized with anti-DNP IgE alone and stimulated with DNP-ALB. The graphs show the percentage of cells displaying CD63$^+$ granules in contact with cortical areas devoid of F-actin in control and p66Shc$^{-/-}$ BMMCs, untreated (black bars) or stimulated as described above (white bars). The data are presented as mean ± SD (n=2; 100 cells/sample).

pairment of β-hexosaminidase release observed in these cells (Supplemental Fig. 1).

As cortical F-actin fragmentation is postulated to promote granule exocytosis, and p66Shc appears to play a key role in this process, we asked whether an increased concentration of granules could be detected in the proximity of cortical F-actin-free regions in p66Shc$^{-/-}$ BMMCs compared with controls. To this end, cells were costained with TRITC-phalloidin and a mAb against the exosome marker CD63 and analyzed by confocal microscopy. A significant increase in the percentage of cells showing CD63$^+$ granules at sites devoid of F-actin was observed in resting p66Shc$^{-/-}$ BMMCs compared with control cells (**Fig. 3**). In addition, confocal images showed that p66Shc$^{-/-}$ in BMMCs results in the aggregation of CD63$^+$ granules close to the plasma membrane, at variance with control cells, which display a largely cytosolic granule distribution. Of note, the plasma membrane localization of CD63$^+$ granules observed in resting p66Shc$^{-/-}$ BMMCs was similar to that observed in control BMMCs following antigen stimulation (Fig. 3). Moreover, p66Shc overexpression in RBL-2H3 cells results in the inability of CD63$^+$ granules to redistribute to the plasma membrane, even following antigen stimulation (data not shown). Together, these data support a role for p66Shc as a critical regulator of vesicle-mediated secretion.

Beside actin rearrangements, microtubule dynamics are required for granule translocation to the plasma membrane [14, 28]. No evident alterations in the microtubule network organization were observed in p66Shc$^{-/-}$ BMMCs or in p66Shc-expressing RBL-2H3 compared with controls, both in resting and in antigen-stimulated conditions, indicating that p66Shc does not affect microtubule dynamics. Accordingly, nocodazole treatment impaired antigen-induced degranulation to a similar extent in p66Shc$^{-/-}$ and control BMMCs, as well as in the RBL-2H3 transfectants (Supplemental Fig. 2).

It is well established that cell-surface F-actin remodeling is required for vesicle trafficking and formation of membrane protrusions [29]. In mast cells, plasma membrane extensions, referred to as ruffles, have been described. These extensions are rich in F-actin, and their number increases following antigen activation [30]. To characterize further the effects of p66Shc on antigen-induced actin reorganization, we used RBL-2H3 cells expressing p66Shc to assess ruffle formation by confocal microscopy. IgE sensitization did not induce ruffle formation compared in either cell transfectant. At variance, antigen treatment promoted the formation of ruffles, which was strongly inhibited by p66Shc (**Fig. 4A**). Furthermore, using a RBL-2H3 cell line expressing a p66Shc-GFP fusion protein, we found a linear correlation between p66Shc expression and the number of cells showing antigen-induced ruffles. Specifically, we used a pool of transfectants consisting of cells expressing p66Shc-GFP at different levels. During confocal analysis, we selected cells expressing (detectable) or not expressing (not detectable) p66Shc-GFP and counted cells showing ruffles. A significantly smaller proportion of cells expressing p66Shc-GFP displayed ruffles compared with cells not expressing p66Shc-GFP (Fig. 4B). In agreement with a specific effect of p66Shc on ruffle formation, we found that in stably transfected RBL-2H3 cells, which homogeneously express p66Shc at high levels, only ~10% of cells were still capable of forming ruffles (Fig. 4A), in contrast with the pool of transfectants consisting of a heterogeneous population in terms of p66Shc-GFP expression, where ~40% of the cells showed ruffles (Fig. 4B). Moreover, we found that LatB completely abrogated ruffle formation in antigen-stimulated p66Shc GFP-negative cells, indicating that this drug mimics the effects of p66Shc in ruffle formation (Fig. 4B).

Consistent with a basal-activated phenotype and with a negative role for p66Shc in controlling F-actin dynamics, unstimulated p66Shc$^{-/-}$ BMMCs showed an increase in the number of ruffles compared with control cells, which reach the level of antigen-stimulated control BMMCs and are not altered by IgE or antigen treatment (see Supplemental Videos 1 and 2, and data not shown). Together, the data indicate that p66Shc is implicated in the F-actin dynamics required for ruffle formation following antigen stimulation in mast cells.

p66Shc impairs FcεRI-dependent phosphorylation of Vav and paxillin

Cortical F-actin fragmentation and formation of filopodia are dependent on RhoA and Cdc42, respectively, whereas formation of lamellipodia and membrane ruffles depends on Rac1. The guanine nucleotide exchanger Vav and the adapter paxillin, which contribute to the activation of these GTPases [31–33], have been implicated in neutrophil degranulation [34]. Furthermore, Vav has been shown to be required for the F-ac-

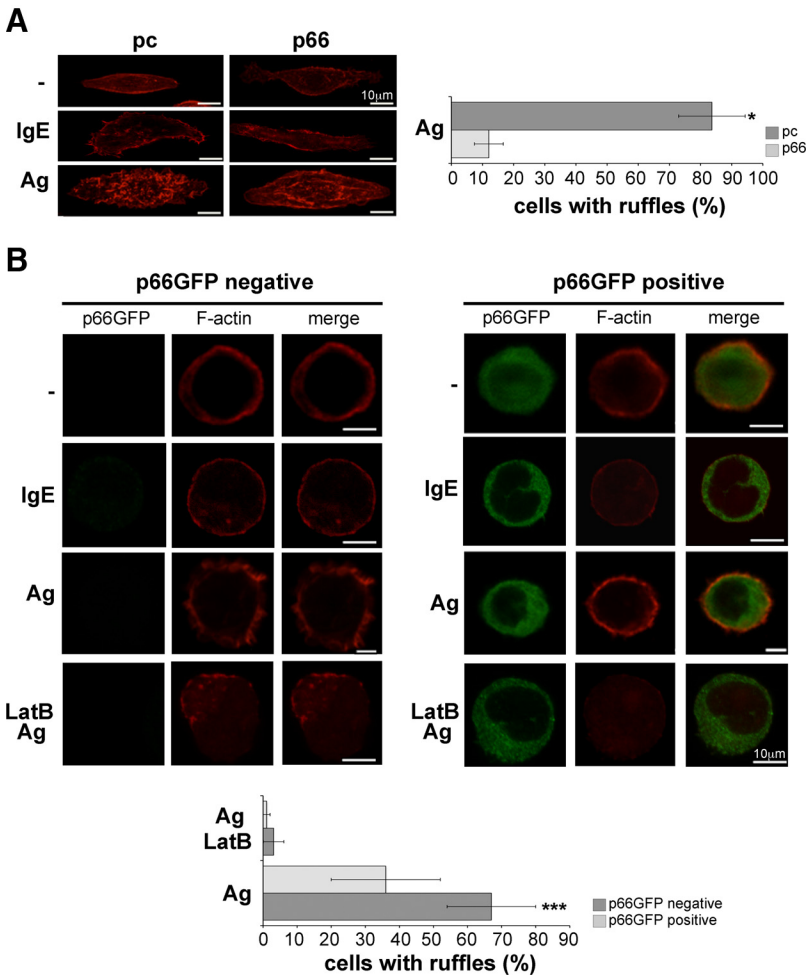

Figure 4. p66Shc impairs membrane ruffling in mast cells. (A) Representative Z-projections (40 slices; slice spacing 0.4 μm) of F-actin distribution of RBL-2H3 cells transfected with the vector pcDNA3 (pc) or with the same vector encoding WT p66Shc (p66). Cells were unstimulated or sensitized with anti-DNP IgE and then stimulated with DNP-ALB and stained with TRITC-labeled phalloidin. The graphs show the percentage of cells displaying ruffle formation following antigen stimulation (n=2; 100 cells/sample). (B) Representative confocal micrographs of F-actin distribution of a pool of RBL-2H3 transfectants expressing (p66GFP positive) or not (p66GFP negative) p66Shc-GFP, unstimulated or stimulated as in A, in the presence (LatB Ag) or absence (Ag) of LatB. The graphs show the quantitation of cells displaying ruffle formation under these conditions (n=2; 200 cells/sample). The data are presented as mean ± SD (cells in each field taken as 100%).

tin rearrangements that control cytotoxic granule release from NK cells [31, 35, 36].

To gain further insight into the mechanism underlying the negative role of p66Shc in antigen-dependent cortical F-actin disassembly, we analyzed the activation status of Vav and paxillin. In agreement with the enhanced secretion observed in p66Shc$^{-/-}$ BMMCs, the lack of p66Shc correlated with a significant enhancement in antigen-induced Vav phosphorylation compared with control BMMCs (**Fig. 5A**). Moreover, the expression of p66Shc in RBL-2H3 cells strongly impaired antigen-dependent Vav phosphorylation (Fig. 5B), indicating that p66Shc acts as an inhibitor of Vav activation in mast cells. Similar results were obtained when paxillin phosphorylation was analyzed in BMMCs from control and p66Shc$^{-/-}$ mice (Fig. 5A). These effects of p66Shc$^{-/-}$ on antigen-dependent Vav and paxillin phosphorylation are likely to underline, at least in part, its ability to negatively regulate the cortical F-actin reorganization required for membrane ruffling and secretion.

We have reported previously that p66Shc recruits the lipid phosphatase SHIP1 to FcεRI [22]. The activation of Vav and paxillin is dependent on phosphoinositides generated by PI3K [37, 38] and indeed, that the cortical actin meshwork has been shown to be associated with a PIP3-enriched compartment of the plasma membrane [39]. Hence, we can hypothe-

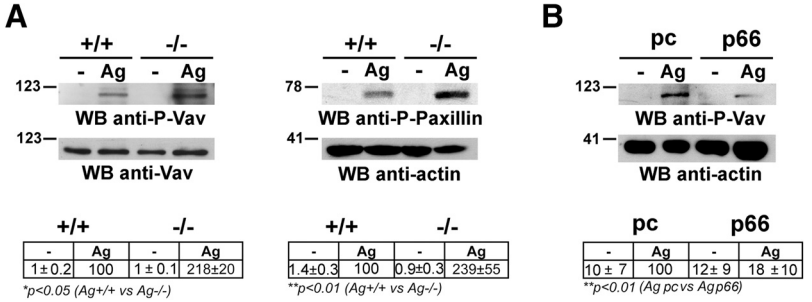

Figure 5. p66Shc impairs Vav and paxillin phosphorylation. Immunoblot analysis of Vav and paxillin phosphorylation (P-Vav and P-Paxillin, respectively) on total cell lysates from control and p66Shc$^{-/-}$ BMMCs (A) or of Vav phosphorylation in control RBL-2H3 cells (pc) and cells expressing p66Shc (p66) (B), untreated or sensitized and stimulated (Ag). Densitometric analysis is shown. Data are presented as relative protein phosphorylation, with the value of antigen-stimulated control cells in each experiment taken as 100% (n=3). WB, Western blot.

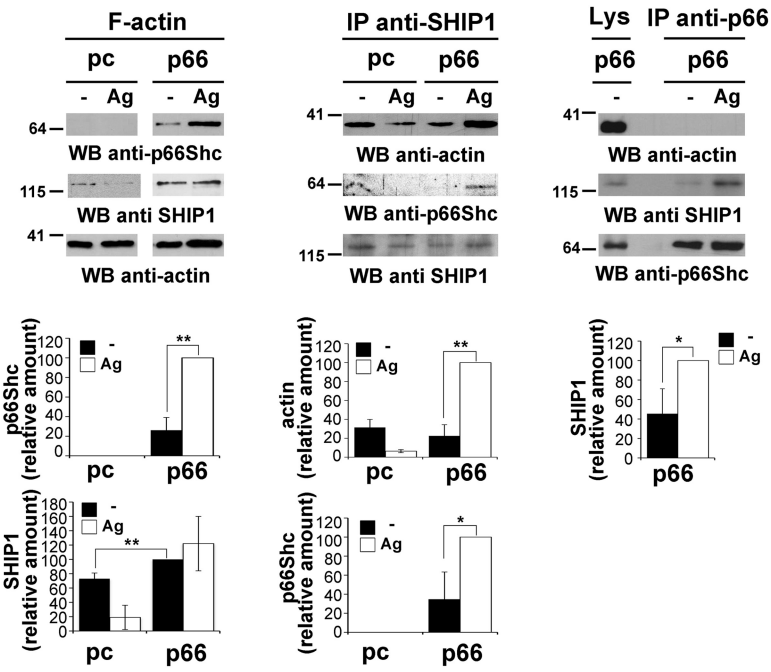

Figure 6. p66Shc is recruited to the F-actin cytoskeleton and impairs antigen-dependent release of SHIP1 from F-actin-rich fractions. Control RBL-2H3 cells (pc) and cells expressing p66Shc (p66) were left untreated or were sensitized and stimulated (Ag) and subjected to F-actin skeleton fractionation (left) or to immunoprecipitation (IP) using anti-SHIP1 (middle) or anti-p66Shc antibodies (right). Immunoblot analyses were performed using the indicated antibodies. A densitometric analysis of p66Shc and SHIP1 localization in the F-actin skeleton fractions (n=2; left), of actin and p66Shc associated with SHIP1 (n=3; middle) and of SHIP1 associated with p66Shc (n=2; right) is also shown.

size that the inhibition of antigen-induced F-actin dynamics could result from p66Shc-dependent inhibition of PIP3-dependent signaling.

p66Shc is recruited to the F-actin cytoskeleton compartment

SHIP1 has been demonstrated to play an important role in the negative regulation of mast cell degranulation by interacting with F-actin through filamin as well as with FcεRI [23, 40]. As p66Shc promotes SHIP1 recruitment to the plasma membrane following FcεRI engagement [22], we asked whether the inhibitory effects of p66Shc on actin remodeling are dependent on its localization to F-actin-rich regions. To address this issue, RBL-2H3-expressing p66Shc and control cells lacking p66Shc expression were left untreated or treated with antigen. F-actin-enriched fractions were prepared from total cell lysates, and the presence of p66Shc and SHIP1 was assessed by immunoblot. At variance with control RBL-2H3 cells, where SHIP1 is excluded from F-actin fractions following antigen stimulation, FcεRI stimulation in p66Shc-expressing RBL-2H3 cells induces p66Shc recruitment to F-actin and SHIP1 stabilization into this fraction (**Fig. 6**, left). In agreement with an inhibitory effect of p66Shc on antigen-dependent release of SHIP1 from F-actin-enriched fractions, the levels of actin and p66Shc found in SHIP1-specific immunoprecipitates were increased in p66Shc-overexpressing cells following antigen stimulation, whereas antigen stimulation induced a reduction in the levels of actin associated with SHIP1 in the control transfectant (Fig. 6, middle). No association of p66Shc with actin was detectable before or following antigen stimulation in p66Shc-specific immunoprecipitates. Conversely, SHIP1 was found to coprecipitate with p66Shc (Fig. 6, right). The finding that p66Shc is associated with the F-actin skeleton in resting cells and that it is further recruited to this compartment following antigen stimulation, together with the evidence of its direct association with SHIP1 but not actin, suggests that p66Shc interacts with F-actin as a complex with SHIP1.

AUTHORSHIP

G.M., D.M., C.T.B., and C.U. designed research and analyzed and interpreted data. G.M., D.M., E.V., E.P., and M.G.R. performed research. P.G.P. and P.L. contributed vital reagents. C.U., G.M., and C.T.B. drafted the manuscript.

ACKNOWLEDGMENTS

This work was supported by grants from Italian Association for Cancer Research (AIRC) and Ministero dell'Istruzione, dell'Università e della Ricerca [MIUR; Programmi di Ricerca di Rilevante Interesse Nazionale (PRIN) and Fondo per gli Investimenti della Ricerca di Base (FIRB)] to C.T.B. The authors thank Marina De Bernard for the generous gift of valuable reagents and Sonia Grassini for technical assistance.

DISCLOSURES

There is no conflict of interest.

REFERENCES

1. Gilfillan, A. M., Tkaczyk, C. (2006) Integrated signalling pathways for mast-cell activation. *Nat. Rev. Immunol.* **6,** 218–230.
2. Galli, S. J., Nakae, S., Tsai, M. (2005) Mast cells in the development of adaptive immune responses. *Nat. Immunol.* **6,** 135–142.
3. Galli, S. J., Tsai, M. (2010) Mast cells in allergy and infection: versatile effector and regulatory cells in innate and adaptive immunity. *Eur. J. Immunol.* **40,** 1843–1851.
4. Shefler, I., Salamon, P., Hershko, A. Y., Mekori, Y. A. (2011) Mast cells as sources and targets of membrane vesicles. *Curr. Pharm. Des.* **17,** 3797–3804.

5. Dvorak, A. M. (2005) Piecemeal degranulation of basophils and mast cells is effected by vesicular transport of stored secretory granule contents. *Chem. Immunol. Allergy* **85,** 135–184.
6. Crivellato, E., Nico, B., Bertelli, E., Nussdorfer, G. G., Ribatti, D. (2006) Dense-core granules in neuroendocrine cells and neurons release their secretory constituents by piecemeal degranulation (review). *Int. J. Mol. Med.* **18,** 1037–1046.
7. Bobrie, A., Colombo, M., Raposo, G., Thery, C. (2011) Exosome secretion: molecular mechanisms and roles in immune responses. *Traffic* **12,** 1659–1668.
8. Kunder, C. A., St John, A. L., Li, G., Leong, K. W., Berwin, B., Staats, H. F., Abraham, S. N. (2009) Mast cell-derived particles deliver peripheral signals to remote lymph nodes. *J. Exp. Med.* **206,** 2455–2467.
9. Gyorgy, B., Szabo, T. G., Pasztoi, M., Pal, Z., Misjak, P., Aradi, B., Laszlo, V., Pallinger, E., Pap, E., Kittel, A., Nagy, G., Falus, A., Buzas, E. I. (2011) Membrane vesicles, current state-of-the-art: emerging role of extracellular vesicles. *Cell. Mol. Life Sci.* **68,** 2667–2688.
10. Taylor, D. D., Gercel-Taylor, C. (2011) Exosomes/microvesicles: mediators of cancer-associated immunosuppressive microenvironments. *Semin. Immunopathol.* **33,** 441–454.
11. Frigeri, L., Apgar, J. R. (1999) The role of actin microfilaments in the down-regulation of the degranulation response in RBL-2H3 mast cells. *J. Immunol.* **162,** 2243–2250.
12. Holowka, D., Sheets, E. D., Baird, B. (2000) Interactions between FcεRI and lipid raft components are regulated by the actin cytoskeleton. *J. Cell Sci.* **113,** 1009–1019.
13. Martin-Verdeaux, S., Pombo, I., Iannascoli, B., Roa, M., Varin-Blank, N., Rivera, J., Blank, U. (2003) Evidence of a role for Munc18-2 and microtubules in mast cell granule exocytosis. *J. Cell Sci.* **116,** 325–334.
14. Nishida, K., Yamasaki, S., Ito, Y., Kabu, K., Hattori, K., Tezuka, T., Nishizumi, H., Kitamura, D., Goitsuka, R., Geha, R. S., Yamamoto, T., Yagi, T., Hirano, T. (2005) FcεRI-mediated mast cell degranulation requires calcium-independent microtubule-dependent translocation of granules to the plasma membrane. *J. Cell Biol.* **170,** 115–126.
15. Holst, J., Sim, A. T., Ludowyke, R. I. (2002) Protein phosphatases 1 and 2A transiently associate with myosin during the peak rate of secretion from mast cells. *Mol. Biol. Cell.* **13,** 1083–1098.
16. Allen, J. D., Jaffer, Z. M., Park, S. J., Burgin, S., Hofmann, C., Sells, M. A., Chen, S., Derr-Yellin, E., Michels, E. G., McDaniel, A., Bessler, W. K., Ingram, D. A., Atkinson, S. J., Travers, J. B., Chernoff, J., Clapp, D. W. (2009) p21-Activated kinase regulates mast cell degranulation via effects on calcium mobilization and cytoskeletal dynamics. *Blood* **113,** 2695–2705.
17. Villanueva, J., Torres, V., Torregrosa-Hetland, C. J., Garcia-Martinez, V., Lopez-Font, I., Viniegra, S., Gutierrez, L. M. (2012) F-Actin-myosin II inhibitors affect chromaffin granule plasma membrane distance and fusion kinetics by retraction of the cytoskeletal cortex. *J. Mol. Neurosci.* **48,** 328–338.
18. Pendleton, A., Koffer, A. (2001) Effects of latrunculin reveal requirements for the actin cytoskeleton during secretion from mast cells. *Cell. Motil. Cytoskeleton* **48,** 37–51.
19. Yu, H. Y., Bement, W. M. (2007) Control of local actin assembly by membrane fusion-dependent compartment mixing. *Nat. Cell Biol.* **9,** 149–159.
20. Malacombe, M., Bader, M. F., Gasman, S. (2006) Exocytosis in neuroendocrine cells: new tasks for actin. *Biochim. Biophys. Acta* **1763,** 1175–1183.
21. Finetti, F., Savino, M. T., Baldari, C. T. (2009) Positive and negative regulation of antigen receptor signaling by the Shc family of protein adapters. *Immunol. Rev.* **232,** 115–134.
22. Ulivieri, C., Fanigliulo, D., Masi, G., Savino, M. T., Gamberucci, A., Pelicci, P. G., Baldari, C. T. (2011) p66Shc is a negative regulator of FcεRI-dependent signaling in mast cells. *J. Immunol.* **186,** 5095–5106.
23. Lesourne, R., Fridman, W. H., Daeron, M. (2005) Dynamic interactions of FcγRIIB with filamin-bound SHIP1 amplify filamentous actin-dependent negative regulation of FcεRI signaling. *J. Immunol.* **174,** 1365–1373.
24. Suzuki, R., Liu, X., Olivera, A., Aguiniga, L., Yamashita, Y., Blank, U., Ambudkar, I., Rivera, J. (2010) Loss of TRPC1-mediated Ca^{2+} influx contributes to impaired degranulation in Fyn-deficient mouse bone marrow-derived mast cells. *J. Leukoc. Biol.* **88,** 863–875.
25. Carroll-Portillo, A., Surviladze, Z., Cambi, A., Lidke, D. S., Wilson, B. S. (2012) Mast cell synapses and exosomes: membrane contacts for information exchange. *Front. Immunol.* **3,** 46.
26. Smalley, D. M., Sheman, N. E., Nelson, K., Theodorescu, D. (2008) Isolation and identification of potential urinary microparticle biomarkers of bladder cancer. *J. Proteome Res.* **7,** 2088–2096.
27. Tumova, M., Koffer, A., Simicek, M., Draberova, L., Draber, P. (2010) The transmembrane adaptor protein NTAL signals to mast cell cytoskeleton via the small GTPase Rho. *Eur. J. Immunol.* **40,** 3235–3245.
28. Hajkova, Z., Bugajev, V., Draberova, E., Vinopal, S., Draberova, L., Janacek, J., Draber, P., Draber, P. (2011) STIM1-directed reorganization of microtubules in activated mast cells. *J. Immunol.* **186,** 913–923.
29. Ridley, A. J. (2006) Rho GTPases and actin dynamics in membrane protrusions and vesicle trafficking. *Trends Cell Biol.* **16,** 522–529.
30. Edgar, A. J., Bennett, J. P. (1997) Circular ruffle formation in rat basophilic leukemia cells in response to antigen stimulation. *Eur. J. Cell Biol.* **73,** 132–140.
31. Lazer, G., Katzav, S. (2011) Guanine nucleotide exchange factors for RhoGTPases: good therapeutic targets for cancer therapy? *Cell. Signal.* **23,** 969–979.
32. Deakin, N. O., Turner, C. E. (2008) Paxillin comes of age. *J. Cell Sci.* **121,** 2435–2444.
33. Wells, C. M., Walmsley, M., Ooi, S., Tybulewicz, V., Ridley, A. J. (2004) Rac1-deficient macrophages exhibit defects in cell spreading and membrane ruffling but not migration. *J. Cell Sci.* **117,** 1259–1268.
34. Kamen, L. A., Schlessinger, J., Lowell, C. A. (2011) Pyk2 is required for neutrophil degranulation and host defense responses to bacterial infection. *J. Immunol.* **186,** 1656–1665.
35. Hornstein, I., Alcover, A., Katzav, S. (2004) Vav proteins, masters of the world of cytoskeleton organization. *Cell. Signal.* **16,** 1–11.
36. Colucci, F., Rosmaraki, E., Bregenholt, S., Samson, S. I., Di Bartolo, V., Turner, M., Vanes, L., Tybulewicz, V., Di Santo, J. P. (2001) Functional dichotomy in natural killer cell signaling: Vav1-dependent and -independent mechanisms. *J. Exp. Med.* **193,** 1413–1424.
37. Robertson, L. K., Mireau, L. R., Ostergaard, H. L. (2005) A role for phosphatidylinositol 3-kinase in TCR-stimulated ERK activation leading to paxillin phosphorylation and CTL degranulation. *J. Immunol.* **175,** 8138–8145.
38. Bhavsar, P. J., Vigorito, E., Turner, M., Ridley, A. J. (2009) Vav GEFs regulate macrophage morphology and adhesion-induced Rac and Rho activation. *Exp. Cell. Res.* **315,** 3345–3358.
39. Konig, I., Schwarz, J. P., Anderson, K. I. (2008) Fluorescence lifetime imaging: association of cortical actin with a PIP3-rich membrane compartment. *Eur. J. Cell Biol.* **87,** 735–741.
40. Gimborn, K., Lessmann, E., Kuppig, S., Krystal, G., Huber, M. (2005) SHIP down-regulates FcεR1-induced degranulation at supraoptimal IgE or antigen levels. *J. Immunol.* **174,** 507–516.

KEY WORDS:
microvesicles · SHIP1 · signal transduction